

Bias Dependence of Non-Fourier Heat Conduction in GaN HEMTs

Yang Shen

Department of Engineering Mechanics, School of Aerospace Engineering,
Tsinghua University

June 29, 2022

Overview

- ⚙ Self-heating in GaN HEMTs can cause reliability issues and degrade the device performance. Being the result of Joule heating, self-heating is highly **bias dependent**.
- ⚙ Previous studies on self-heating are mainly based on Fourier's law of heat conduction, **the non-Fourier effects have not been studied quantitatively**.
- ⚙ We reexamined the bias dependence of self-heating in GaN HEMTs by **TCAD and hybrid Monte Carlo-diffusion simulations**, and developed a semi-empirical thermal resistance model which can **take the bias dependence and phonon transport into account**.

1 Introduction

- Self-Heating in GaN HEMTs
- Bias Dependence of Self-Heating
- Phonon Ballistic Transport in GaN HEMTs

2 Device Structure and Simulation Details

3 Results and Discussion

4 Remaining Work

5 Program Development

Thermal Issues in GaN HEMTs

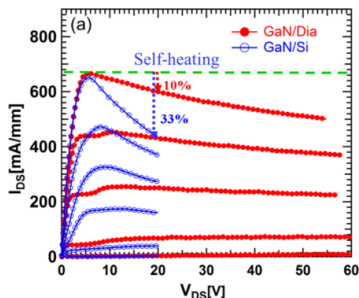


Figure 1: $I_{DS} - V_{DS}$ of GaN/Dia and GaN/Si HEMTs ³.

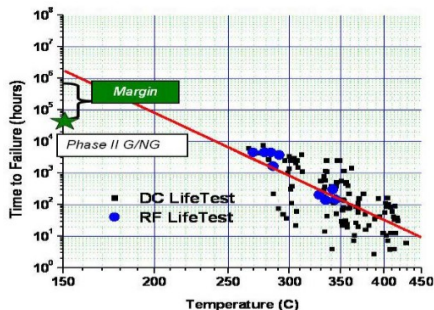


Figure 2: Mean time to failure (MTTF) for TriQuint GaN PAs ⁴.

The significant overheating within the devices largely **degrades the electrical performance** and **shortens the device lifetime**.

¹K. Ranjan, S. Arulkumaran, G. Ng, *et al.*, "Investigation of self-heating effect on dc and rf performances in algan/gan hemts on cvd-diamond," *IEEE Journal of the Electron Devices Society*, vol. 7, pp. 1264–1269, 2019.

²M. Rosker, C. Bozada, H. Dietrich, *et al.*, "The darpa wide band gap semiconductors for rf applications (wbgs-rf) program: Phase ii results," *CS ManTech*, vol. 1, pp. 1–4, 2009.

Bias Dependence of Self-Heating

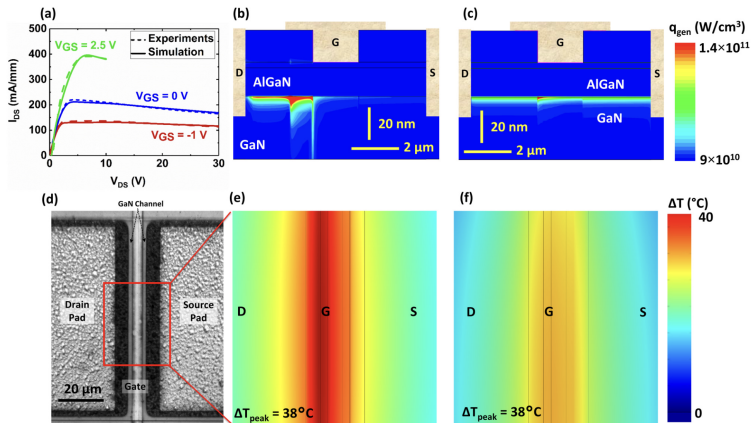


Figure 3: Bias dependent results for channel conditions with $V_{GS} = -1$ V and $V_{GS} = 2.5$ V, respectively³, $P_{diss} = 250$ mW.

³B. Chatterjee, C. Dundar, T. E. Beechem, *et al.*, "Nanoscale electro-thermal interactions in algan/gan high electron mobility transistors," *Journal of Applied Physics*, vol. 127, no. 4, p. 044 502, 2020.

Two Heat Source Model⁴

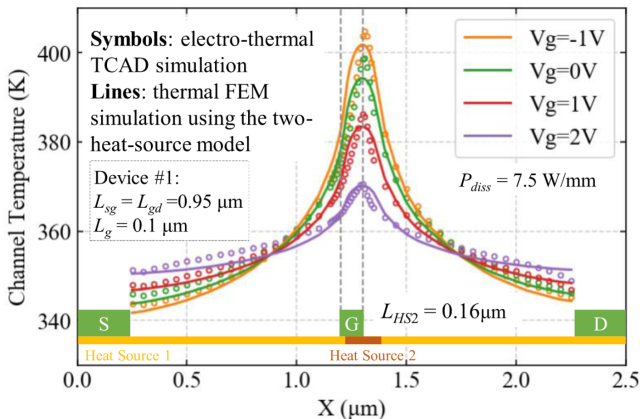


Figure 4: Temperature profiles across the channel at $P_{diss} = 7.5 \text{ W/mm}$ and the four different biases.

⁴X. Chen, S. Boumaiza, and L. Wei, "Modeling bias dependence of self-heating in gan hems using two heat sources," *IEEE Transactions on Electron Devices*, vol. 67, no. 8, pp. 3082–3087, 2020.

Phonon Ballistic Transport

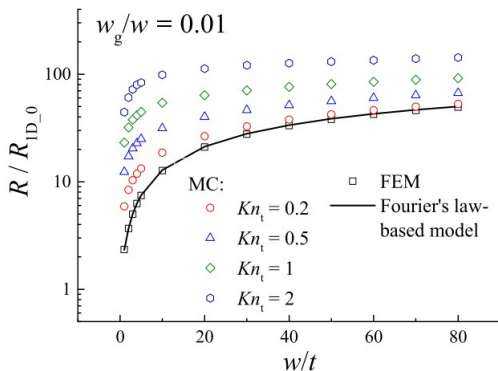



Figure 5: Dimensionless total thermal resistance as a function of w/t , with $w_g/w = 0.005$ and 0.01 ⁵.

Phonon Ballistic Transport can significantly increase the thermal resistance.


⁵Y.-C. Hua, H.-L. Li, and B.-Y. Cao, "Thermal spreading resistance in ballistic-diffusive regime for gan hemts," *IEEE Transactions on Electron Devices*, vol. 66, no. 8, pp. 3296–3301, 2019.

This Work

Motivation

-  Reexamine the self-heating effects in GaN HEMTs with the consideration of phonon ballistic transport.

This Work

-  **TCAD and hybrid Monte Carlo-diffusion simulations** were conducted to study the self-heating effects in GaN HEMTs, the two-heat-source model was improved to take the ballistic effects into consideration.

1 Introduction

2 Device Structure and Simulation Details

- Device Structure and TCAD Setup
- Phonon Monte Carlo Simulation

3 Results and Discussion

4 Remaining Work

5 Program Development

Device Structure⁶

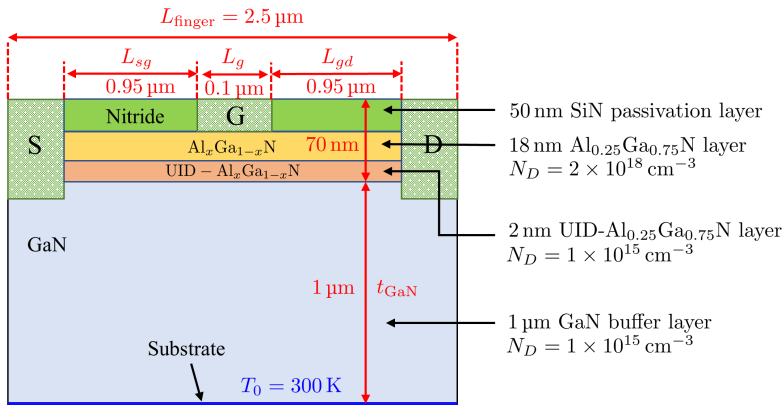


Figure 6: Schematic of GaN HEMT. The geometries are not drawn to scale.

⁶X. Chen, S. Boumaiza, and L. Wei, "Self-heating and equivalent channel temperature in short gate length gan hems," *IEEE transactions on electron devices*, vol. 66, no. 9, pp. 3748–3755, 2019.

Output Characteristics

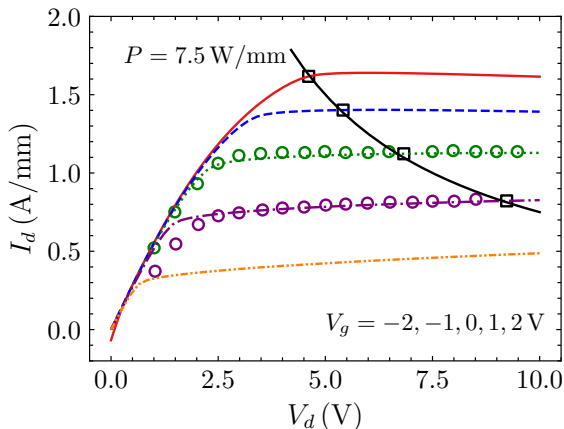


Figure 7: Output characteristics of the HEMT under V_g from -2 V to 2 V with an interval of 1 V .

Bias-Dependent Heat Generation

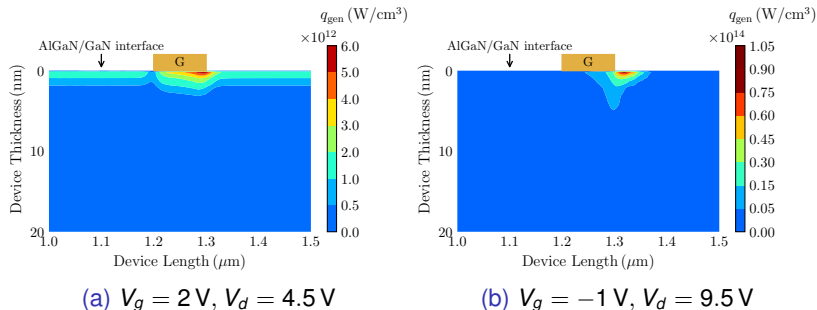


Figure 8: The total power dissipation level for the two bias conditions, $P = 7.5\text{ W}/\text{mm}$.

Phonon Monte Carlo Simulation

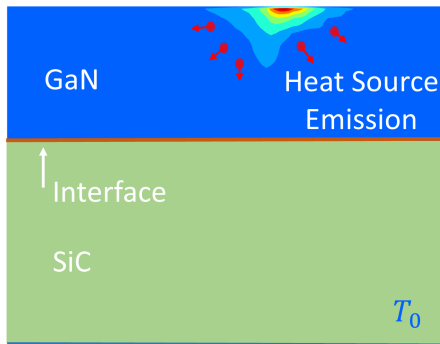


Figure 9: Schematic diagram of the simulated GaN HEMT, the Juole heating profile calculated by TCAD is imported to MC simulations as heat source.

Phonon Dispersion

- An isotropic sine-shaped phonon dispersion (Born-von Karman dispersion) is used.
- Longitudinal and transverse branches are not differentiated.

$$\omega(k) = \omega_{\max} \sin(\pi k / 2k_m)$$

$$k_m = \left(\frac{6\pi^2 N}{V} \right)^{1/3}, \quad a = \pi / k_m, \quad \omega_m = 2v_{0g} / a$$

Relaxation time

Matthiessen's rule:

$$\tau^{-1} = \tau_{impurity}^{-1} + \tau_U^{-1} = A\omega^4 + B\omega^2 T \exp(-C/T)$$

Thermal conductivity fitting:

$$\mathcal{L}(A, B, C) = \sum_p \left\| \frac{1}{3} \sum_p \int_0^{\omega_m} C_\omega v_\omega l_\omega d\omega - k_{exp} \right\|^2$$

$$C(\omega, p) = \hbar\omega D(\omega, p) \frac{\partial f^{BE}}{\partial T} = \hbar\omega \frac{\kappa^2}{2\pi^2 |v_g|} \frac{\hbar\omega e^{\frac{\hbar\omega}{T k_B}}}{T^2 k_B \left(e^{\frac{\hbar\omega}{T k_B}} - 1 \right)^2}$$

Phonon Dispersion and Relaxation time

Table 1: Fitted phonon dispersion and scattering parameters⁷.

Parameter (Unit)	GaN	SiC
$k_0 (1 \times 10^9 \text{ m}^{-1})$	10.94	8.94
$\omega_m (1 \times 10^{13} \text{ rad/s})$	3.50	7.12
$a_D (\text{\AA})$	2.87	3.51
$A (1 \times 10^{-45} \text{ s}^3)$	5.26	1.00
$B (1 \times 10^{-19} \text{ s/K})$	1.10	0.596
$C (\text{K})$	200	235.0

⁷Q. Hao, H. Zhao, and Y. Xiao, "A hybrid simulation technique for electrothermal studies of two-dimensional gan-on-sic high electron mobility transistors," *Journal of Applied Physics*, vol. 121, no. 20, p. 204 501, 2017.

Phonon Dispersion and Relaxation time

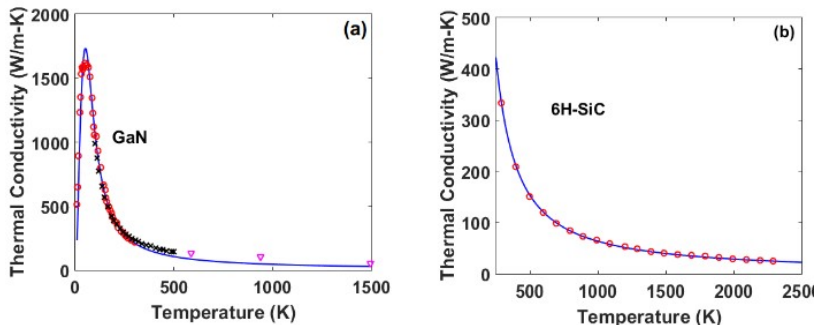


Figure 10: Thermal conductivity from model calculations (line), and from experiments (symbols)⁸.

⁸Q. Hao, H. Zhao, Y. Xiao, *et al.*, "Multi-length scale thermal simulations of gan-on-sic high electron mobility transistors," in *Multiscale Thermal Transport in Energy Systems*, Nova Science Publishers, 2016.

Interface Phonon Transport

Based on **diffuse mismatch model (DMM)**, phonons are diffusively transmitted or reflected by an interface.

The frequency-dependent phonon transmissivity from material 1 to 2 is given as

$$\tau_{12}(\omega) = \frac{\sum_p v_{2,g,p}(\omega) D_{2,p}(\omega)}{\sum_p v_{1,g,p}(\omega) D_{1,p}(\omega) + \sum_p v_{2,g,p}(\omega) D_{2,p}(\omega)}$$

The thermal boundary resistance (TBR) can be further calculated by

$$R = \frac{4}{\int T_{12} C_1(\omega) v_1(\omega) d\omega}$$

Validation of MC Code

Table 2: TBR of GaN/SiC predicted by DMM and MC simulations
(Unit: $\text{m}^2\text{K}/\text{GW}$)

DMM	Heat flux heating		Temperature difference heating	
	GaN emission	SiC emission	GaN emission	SiC emission
23.20	19.23	20.30	19.06	18.16

- 1 Introduction
- 2 Device Structure and Simulation Details
- 3 Results and Discussion**
- 4 Remaining Work
- 5 Program Development

MC Simulations at Different Bias

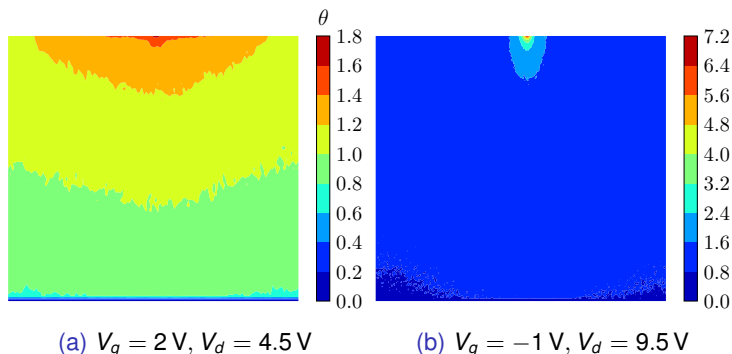


Figure 11: Dimensionless temperature distribution predicted by MC simulations.

- 1 Introduction
- 2 Device Structure and Simulation Details
- 3 Results and Discussion
- 4 Remaining Work**
- 5 Program Development

Remaining Work

- ⚙ Figure out the **simulation size dependence of the results**, ensuring the validity of the simulation.
- ⚙ Develop automated and parametric analysis process.
- ⚙ Carry out TCAD simulations with **different gate lengths**.
- ⚙ Investigate the **hybrid algorithm with phonon dispersion considered**, *e.g.* the selection of the size of different sections.
- ⚙ Current work and previous work are all based on **small temperature difference approximation**, thus the thermal resistance model is **power independent**. detailed analysis and necessary model corrections have to be done in the future, *e.g.* importing $f(P)$ to the model.

- 1 Introduction
- 2 Device Structure and Simulation Details
- 3 Results and Discussion
- 4 Remaining Work
- 5 Program Development**

Python-based 2D Ray-tracing Phonon MC Code

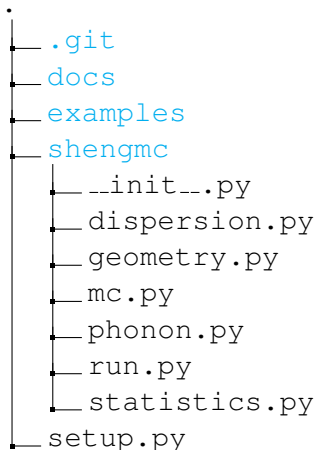


Figure 12: Directory tree of **shengmc**.

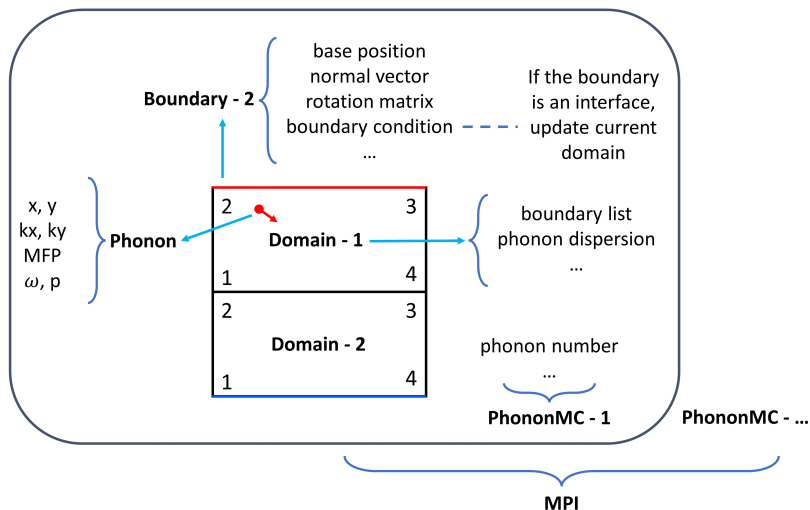


Figure 13: Schematic diagram of **shengmc**.

Inclined Interface

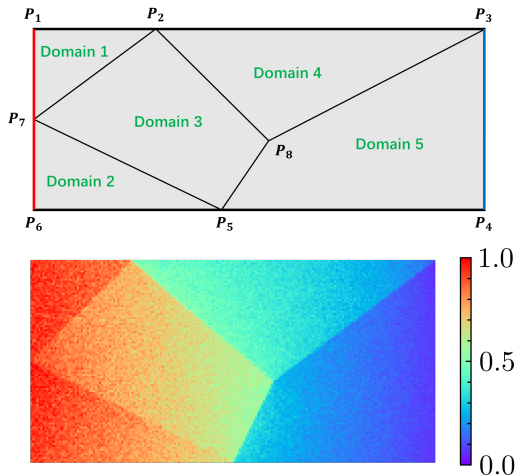


Figure 14: Simulation of a tangram like system.

Multiple Interfaces With Phonon Dispersion

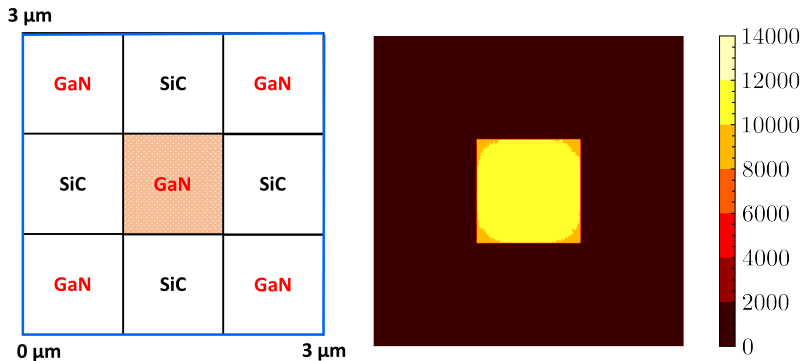


Figure 15: Simulation of a grid like system.

Non-uniform Heat Source

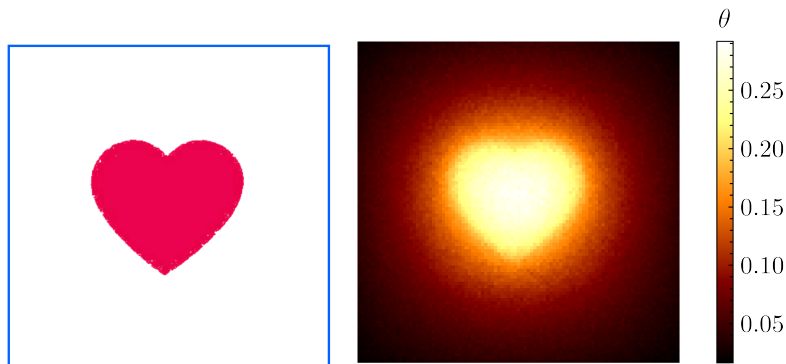


Figure 16: Simulation of a system with non-uniform heat source.

Internal Hole

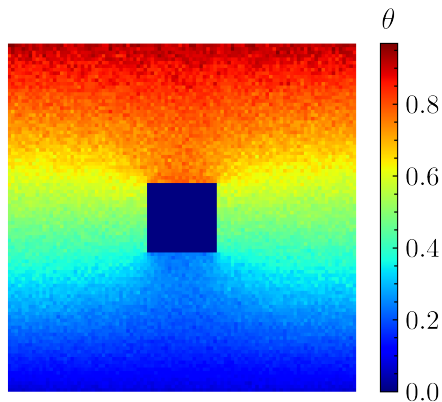


Figure 17: Simulation of a system with an internal hole.

Prospective Features

- 🔗 Support the cross-scale module for device level simulations.

Thank You! 